Energy Coupling in the PSI−LHCI Supercomplex from the Green Alga *Chlamydomonas reinhardtii*[†,||]

Alexander N. Melkozernov,[‡]* Joanna Kargul,[§] Su Lin,[‡] James Barber,[§] and Robert E. Blankenship[‡]

Department of Chemistry and Biochemistry and Center for the Study of Early Events in Photosynthesis, Arizona State University, Tempe, Arizona 85287-1604, and Wolfson Laboratories, Department of Biological Sciences, Imperial College, London SW7 2AY, U.K.

Received: February 11, 2004; In Final Form: April 5, 2004

Energy transfer and trapping in the PSI−LHCI supercomplex from the green alga *Chlamydomonas reinhardtii* have been studied using femtosecond transient absorption and picosecond fluorescence spectroscopy at room temperature. Data suggest that excitations of the PSI−LHCI supercomplex at 700 nm have similar probabilities of excitation of either the primary donor in the PSI core (absorbing at 697 nm) or low-energy Chls in the LHCI (red pigments) that presumably absorb at this spectral region. Both transient absorption and picosecond fluorescence spectroscopy indicate a biphasic overall decay of the excitation in the PSI−LHCI. The process includes a photochemical trapping in the PSI core antenna occurring with a typical lifetime of 25 ± 3 ps and a significantly slower excitation decay phase in the PSI−LHCI supercomplex occurring with a lifetime of 104 ± 20 ps and maximum of absorption changes around 685 nm. The slow excitation decay process suggests presence of an energy transfer pathway from the LHCI to the PSI core, which introduces a diffusion-limited step, in contrast to optimized and energetically well coupled excitation dynamics in the PSI core and CP43′−PSI supercomplexes from iron−stress-induced cyanobacteria. Although LHCI in green algae seems to be similar to those isolated from higher plants the data demonstrate apparent differences in the excitation dynamics suggesting differences in molecular organizations and causes of the red spectral shift associated with PSI. Data of time-resolved spectroscopy are discussed based on the available structural models of PSI−LHCI supercomplexes.

Introduction

In photosynthetic membranes of cyanobacteria, green algae, and higher plants, photosystem I (PSI) carries out a light-driven transmembrane electron transfer from plastocyanin (or cytochrome *c*) to ferredoxin oxidoreductase. An excited state of the primary electron donor, a Chl *a* dimer P700, sensitizes this process. A general feature of all PSI is a structural fusion of the core antenna and the electron-transfer cofactors of the reaction center (RC).[1,2] The PSI core antenna efficiently delivers the captured solar energy to the reaction center via a network of Chl *a* molecules.[3−6] Peripheral light-harvesting antennae that the PSI core has acquired during the course of evolution reveal significant structural diversity ranging from externally coupled phycobilisomes[7,8] or integral membrane iron−stress-induced Chl *a* binding proteins in cyanobacteria[9,10] to integral Chl *a/b* binding LHCI in green algae and higher plants.[2,11,12] An adaptive increase in light-harvesting capacity and absorption cross-section is the major function of the peripheral antenna system.

Excitation dynamics in the PSI core monomers and trimers have been intensively studied during the past decade (reviewed in refs 3 and 4). The PS I core antenna provides effective light harvesting in a broad spectral range (carotenoids + chlorophyll *a* spectral forms including red pigments). The loss-free delivery of the excitation from the core antenna to the reaction center occurs with a lifetime of 20−40 ps.[3,4]

The structural complexity of the PSI−LHCI supercomplex results in an increased kinetic heterogeneity associated with variability in lifetimes of excitation energy transfer processes and the photochemical trapping.[13−18] Such a heterogeneity was suggested to result from a weaker structural coupling of the LHCI antenna and the PSI core as compared to the tight association of the ring of 18 CP43-like iron-stress induced proteins around the PSI trimer in cyanobacteria.[19] In the latter system with a three time larger antenna size the energy transfer from the peripheral antenna (ring of CP43′ or IsiA proteins) to the PSI core was reported to occur on the time scale of several picoseconds, which is much faster than the photochemical trapping of the CP43′−PSI supercomplex (40 ps).[19]

The recent 4.4 Å resolution crystal structure of the PSI−LHCI from pea[2] confirmed that the structure of the PSI core complex in higher plants is largely similar to the structure of the PSI from cyanobacteria determined with a 2.5 Å resolution.[1,20] The two largest transmembrane subunits, PsaA and PsaB, bind 96 Chl *a* molecules and 22 β-carotenes, thus forming an antenna network with optimal energy connectivity around the electron-transfer cofactors of the reaction center.[5,6] The PSI cores from higher plants and green algae have four additional

[†] Part of the special issue "Gerald Small Festschrift".

* To whom correspondence should be addressed. Telephone: (480) 965−1437. Fax: (480) 965−2747. E-mail: alexander.melkozernov@asu.edu.

[‡] Arizona State University.

[§] Imperial College.

[||] Abbreviations: Chl *a*, chlorophyll *a*; Chl *b*, chlorophyll *b*; Δ*A*, absorbance changes; DAS, decay associated spectrum; FDAS, fluorescence decay associated spectrum; fwhm, full-width at half-maximum; IRF, instrument response function; LHCI, light-harvesting complex I; ND, nondecaying component; PB, photobleaching; PSI, photosystem I; PSII, photosystem II; P700, primary electron donor in photosystem I; RC, reaction center.

10.1021/jp049375n CCC: $27.50
Published on Web 05/26/2004

subunits (PsaG, PsaH, PsaN, and PsaO) that most likely reflect the structural coupling of the PSI core with the peripheral antenna.[2,21−23] In contrast to earlier estimates of the size of the complex,[21,24] the crystal structure identified a layer of four monomeric LHCI proteins that are in structural contact with the peripheral subunits of the PSI core, PsaG, PsaF, PsaJ, and PsaK. The crystal structure predicted an asymmetry in the strength of the PSI-to-LHCI binding with the tightest helix−helix interaction between one LHCI monomer (assigned to Lhca1) and the PsaG subunit. Extra Chls have been found between the interacting Lhca proteins in the peripheral antenna and between the LHCI layer and the PSI core surface.

Earlier time-resolved spectroscopy studies of the LHCI monomers from higher plants[3] revealed that Chl *b* to Chl *a* energy transfer in the LHCI occurs largely on the subpicosecond time scale. Within picoseconds, the excitation redistributes among the major Chl *a* spectral forms with significant localization of the excitation on the red pigments in the 680−710 nm spectral region. For LHCI proteins from higher plants, these Chl *a* species determine a significant red spectral shift of the steady-state fluorescence maximum in the region from 702 to 730 nm depending on the type of the Lhca proteins associated with LHCI.[25−28] The excitation energy transfer components with lifetimes varying in the range of 15−30 ps were observed in the LHCI dimers in vitro both by time-resolved absorption[3] and fluorescence spectroscopy.[29,30] This energy transfer process was ascribed to intersubunit energy redistribution within the LHCI dimers.

Earlier in vivo analysis of the steady-state fluorescence in Lhca1- and Lhca4-deleted PSI from barley[31] suggested that the additional red shift of the fluorescence might occur in the PSI−LHCI due to interactions of the Lhca proteins with the surface of the PSI. The extra Chls found on the interface between the LHCI layer and the PSI surface might be involved in these interactions.[2] In the LHCI and the PSI−LHCI from higher plants, the red pigments were found to possess unusual kinetic properties resulting in the thermally activated uphill energy transfer from the red pigments to the PSI core antenna.[32] Earlier fluorescence studies on whole leaves in green plants[33] concluded that up to 80% of the fluorescence in the PSI−LHCI complex originates from the red spectral forms. The uphill energy transfer from the red pigments in the LHCI to the reaction center has a lifetime that is significantly slower than the photochemical trapping in the PSI core antenna[16,32] suggesting that the energy transfer from these red pigments to the PSI core antenna would limit the excitation dynamics of the PSI−LHCI supercomplex in higher plants. This diffusion-limited kinetics resulted from structural association of the LHCI with the PSI core is in contrast to energetically optimized and well-coupled excitation dynamics in the PSI core.[3,5,6,34]

Structural details of the PSI−LHCI from green algae are unknown. The available low-resolution electron microscopy based models of *Chlamydomonas reinhardtii*[11,12] predict binding of 11−14 Lhca proteins. The antenna size of this complex is significantly larger than observed in the crystals of the PSI−LHCI from pea.[2] Low-temperature emission of the PSI−LHCI from *C. reinhardtii* has a maximum at 715 nm in contrast to the 735 nm peak in the PSI−LHCI from higher plants. This suggests possible differences in molecular organizations of the low-energy absorbing pigments and their energy coupling to the PSI core.

In this paper, we present results of a time-resolved spectroscopic study of the PSI−LHCI supercomplex from the green alga *C. reinhardtii* at room temperature. The laser excitation of the supercomplex at 700 nm has been chosen to probe the energy coupling of the peripheral LHCI antenna to the PSI core antenna. The data of femtosecond absorption and picosecond fluorescence spectroscopy demonstrate that the LHCI and the PSI core antenna in the supercomplex are largely isoenergetic. We found that in addition to the photochemical trapping in the PSI core with a typical lifetime of 25 ± 3 ps there is a significantly slower excitation decay phase in the PSI−LHCI supercomplex occurring with a lifetime of 104 ± 20 ps and maximum of absorbance changes at 685 nm. Data indicate that the process involves also the low-energy-absorbing Chls; however, their number in the PSI−LHCI from *C. reinhardtii* is significantly lower than in the higher plant PSI−LHCI.

Materials and Methods

Isolation of PSI Complexes. The PSI−LHCI supercomplexes were isolated from cells of the mutant strain of *C. reinhardtii* with 6His-tag fused with D2 protein[35] using a procedure described in details by Kargul and co-workers.[12] Briefly, isolated thylakoid membranes (0.8 mg Chl/mL) were solubilized with detergents (0.9% (w/v) β-D-dodecylmaltoside (DDM)) and then depleted of His-tagged PSII using Ni−NTA (Qiagen) affinity chromatography. After that the mixture was subjected to 0.1−1 M sucrose gradient centrifugation in a buffer containing 5 mM Tricine-NaOH (pH 8), 0.05% β-dodecylmaltoside, and 0.5 M betaine. The PSI−LHCI supercomplexes were observed in the lowest, most dense green fraction of the gradient. PSI core particles were isolated by further solubilization of the supercomplexes (0.3 mg Chl/mL) with 1.5% β-dodecylmaltoside and 0.6% Zwittergent 3-16 and a sucrose gradient centrifugation of the detergent-treated complexes.[36,37]

Transient Absorption Spectroscopy. For time-resolved absorption spectroscopy, the samples were resuspended in 5 mM Tricine−NaOH pH 8.0, 0.5 M betaine 0.05% β-dodecylmaltoside, 20 mM Na ascorbate, and 20 μM phenazine metasulfate. The sample was loaded in an optical wheel with a path length of 1.2 mm. The rotating rate of the optical cell (5−8 rev/s) and recombination times of reduced acceptors were adjusted to prevent the accumulation of the $P700^+$ during the measurements. The absorbance of the sample in the cell was $\sim 1-1.2$ at the peak of the Q_y absorption band. Transient absorption difference spectra of the PSI−LHCI and the PSI core were measured at room temperature using the femtosecond instrument and techniques described earlier.[38] Briefly, the samples were excited at 700 nm with 200 fs laser pulses (fwhm = 5 nm) with repetition rate of 1 kHz and energy less than 0.5 μJ or 0.94×10^{14} photon pulse^{-1} cm^{-2}. Transient absorption difference (ΔA) spectra of the samples were collected in the 600−750 nm region on a time scale from −1 to +9 ps with a 0.095 ps step of a pump−probe delay and from 9 to 210 ps with a 2 ps step of a pump−probe delay. With resolutions of 0.14 nm per pixel of the dual array detector, the spectral curves were smoothed by averaging of every seven data points resulting in a wavelength step of 1 nm. The analysis of the kinetic data included correction for dispersion, convolution with the instrument response function of the experimental setup (fwhm = 300 fs) and global analysis based on a model of exponential decay of Chl excited states.[38] Global fitting was performed using locally written software ASUFIT (URL: www.public.asu.edu/~laserweb/asufit/asufit.html).

Picosecond Fluorescence Spectroscopy. Time-resolved fluorescence of the PSI core particles and the PSI−LHCI supercomplexes were measured using the time-correlated single-photon counting technique as described earlier.[19] For room-temperature measurements samples were diluted in the buffer

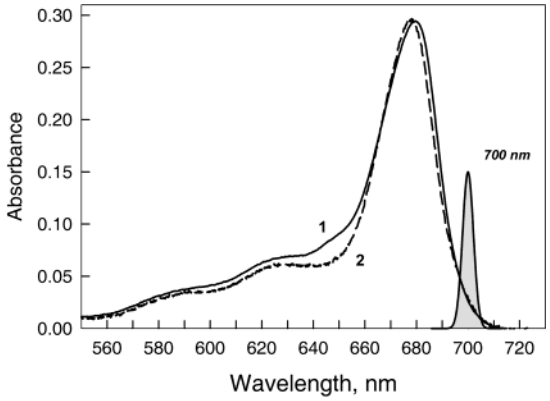

Figure 1. Ground-state absorption spectra of the PSI−LHCI supercomplex (1) and PSI core particles (2) isolated from the green alga *C. reinhardtii*. Spectra measured at room temperature. Shaded in gray is a spectral profile of the laser pulse (fwhm = 5 nm) used for the excitation of the PSI−LHCI and the PSI core at 700 nm. Absorption spectra are normalized at their maxima.

to a final OD of about 0.1 cm^{-1}. The samples were excited at 600 nm with ∼10 ps laser pulses and a repetition rate of 7.6 MHz. To avoid singlet−singlet annihilation intensity of the laser excitation was attenuated to less than $5 \cdot 10^{10}$ photons/cm^2/pulse. The observed kinetics measured with a 5 or 10 nm step in a 640−780 nm region were deconvoluted with an instrument response function (fwhm ≈ 100 ps) and fitted to a sum of exponentials $\sum A_i \exp(-t/\tau_i)$, where A_i and τ_i are the relative amplitude and lifetime of the ith exponential component, respectively. The quality of the global fit was judged by weighted residuals and the global χ^2 parameter. The fluorescence kinetics were analyzed globally, and fluorescence decay associated spectra (FDAS) were constructed as a preexponential component plotted against emission wavelength with positive and negative amplitudes in DAS reflecting a fluorescence decay and a fluorescence rise, respectively. The fit amplitudes were scaled to the steady-state fluorescence intensity by setting the sum of the products of the amplitudes and the lifetimes equal to the intensity, $\sum_i A_i \tau_i$, at each detection wavelength as in ref 19.

Results

Ground State Absorption Spectra of PSI—LHCI and the PSI Core at 297 K. Figure 1 compares ground-state absorption spectra of the PSI−LHCI supercomplex (curve 1) and the PSI core antenna (curve 2) from *C. reinhardtii* in the region of Q_y transitions of Chl *a* and Chl *b*. The major Q_y absorption band of Chl *a* in the PSI−LHCI supercomplex has a maximum at 680 nm. The observed width of the band is due to an overlap of a series of Chl *a* spectral forms in the PSI core antenna (maximum at 678 nm) and in the LHCI antenna (maximum at ∼676−680 nm), as well as Chl *b* from LHCI (650 nm). Two broad unstructured absorption bands at 625 and 590 nm represent 0−1 and 0−2 vibronic transitions of Chls, respectively. In the absorption spectrum of the PSI core, the maximum of the major Q_y absorption band of Chl *a* is 2 nm blue shifted relative to the absorption maximum of the PSI−LHCI. We attribute the observed shift to disruption of the PSI−LHCI connections during the PSI core isolation (see Discussion below). A decrease in absorption around 640−650 nm is due to a lack of Chl *b*. Both PSI core and the PSI−LHCI demonstrate a significant decrease in oscillator strengths of the absorption bands of the low-energy Chls (red pigments) above 700 nm in a striking difference from the cyanobacterial PSI core[40] or PSI−LHCI from higher plants.[32]

Transient Absorption Difference Spectra of the PSI—LHCI Supercomplexes. Figure 2 presents transient absorption difference spectra of the PSI−LHCI complexes excited at 700 nm and measured at 297 K. Excitation at 700 nm results in photobleaching of Chl *a* species absorbing in this spectral region, namely, the primary donor in the PSI RC and long wavelength absorbing antenna Chls in the PSI core and LHCI. Transient ΔA spectra detected at early times after the excitation (Figure 2A) illustrate the complexity of the kinetic processes on the subpicosecond time scale. Initial amplitudes of the photobleaching (PB) in ΔA spectra detected with pump−probe delays from 0 to 0.5 ps are determined by overlap in time of the pump and probe pulses with fwhm = 300 fs. The spectral profile of the excitation pulse at 700 nm has a width of ∼ 100 cm^{-1} (∼5 nm). ΔA spectra at 0.19 and 0.28 ps are broad (fwhm of ∼420 cm^{-1} or 20 nm) and characterized by two ΔA peaks at 697 and 686 nm. Photobleaching of a series of absorption bands in a broad spectral region in response to excitation at 700 nm with a relatively narrow laser pulse in the early transient ΔA spectra is indicative of excitonic interaction of Chl *a* species absorbing in this spectral region. At later times (see 0.28 and 0.57 ps spectra in Figure 2A) the dynamics are characterized by a buildup of the spectral asymmetry in transient spectra toward

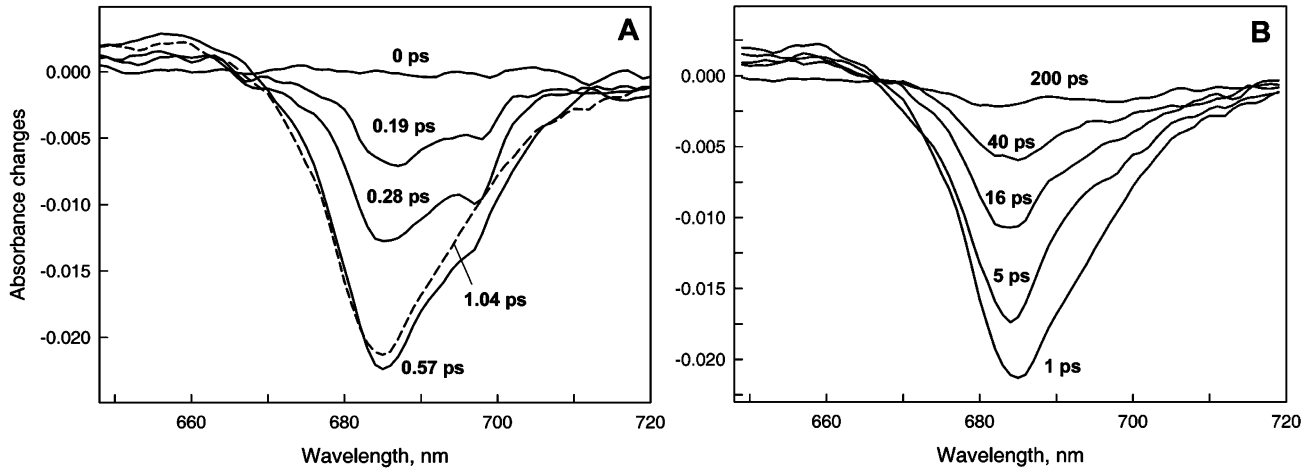

Figure 2. Transient difference absorption spectra of the PSI−LHCI supercomplex measured at 297 K on a 200 ps time scale with excitation at 700 nm. (A) ΔA spectra within 1.04 ps after the excitation. (B) ΔA decay within 210 ps after the excitation. The spectra are shown at different representative pump−probe delays. The level of spectral noise is about 0.002 ΔA.

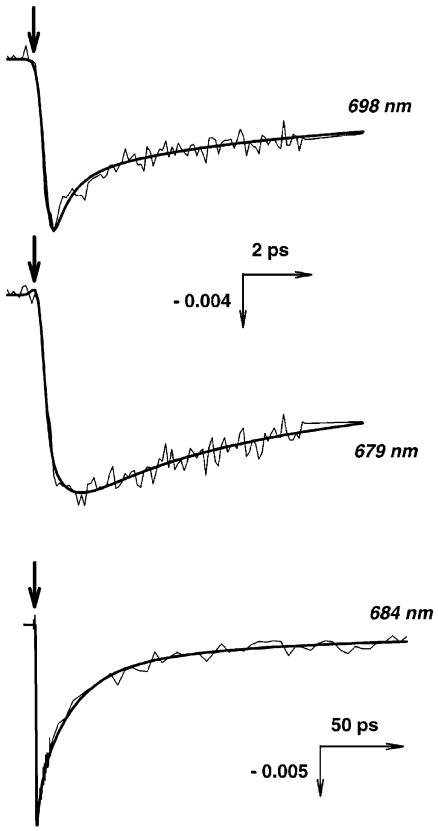

Figure 3. Transient kinetics of absorption changes in the PSI−LHCI supercomplex excited at 700 nm. Kinetics are shown at representative wavelengths on the time scale of 10 ps (ΔA_{698} and ΔA_{679}) and 200 ps (ΔA_{684}). Thick solid lines represent fits based on the multiexponential model (see decay associated spectra in Figure 4).

higher energy relative to excitation wavelength, indicating a dominant uphill energy transfer on the subpicosecond time scale. This is seen in the ΔA kinetics in Figure 3 as a subpicosecond decay of PB at 698 nm and a rise of PB at 679 nm.

The overall decay of the excitation shown in Figure 2B (see also kinetics at 684 nm in Figure 3) reveals a spectral asymmetry of the transient ΔA bands toward the red side from the excitation wavelength. This is associated with a buildup of the PB band of the low-energy-absorbing pigments in the LHCI on the picosecond time scale. On the longer time scale the decay of the excitation in the major pool of Chl *a* reveals two ΔA bands at 697 and 683 nm (see the ΔA spectra at 200 ps). The absorption changes on the longer time scale are largely due to P700 photooxidation with maximum of photobleaching at 697 nm (characteristic of the PSI from *C. reinhardtii*) although these changes are overlapped with ongoing slower decay of the Chl *a* photobleaching in the LHCI antenna around 680 nm (see residual ΔA at 200 ps in the ΔA_{684} kinetics in Figure 3).

Global analysis of the time-resolved data helps to distinguish at least four kinetic processes observed in the PSI−LHCI supercomplexes on the time scales from hundreds of femtoseconds to nanoseconds. Decay associated spectra (DAS) in Figure 4 illustrate the spectral profile of the initial amplitudes of the exponential components with lifetimes of 0.5 ± 0.1, 2.3 ± 0.7, 20 ± 3, 104 ± 20 ps and a long-lived component that is nondecaying on the time scale of the study.

The time resolution of the femtosecond instrument (IRF of ~300 fs) does not allow one to reliably determine the kinetic phase that describes the spectral broadening in the early transient absorption difference spectra (see 0.19 ps transients in Figure 2A). The shortest observed component (see 0.51 ps DAS in

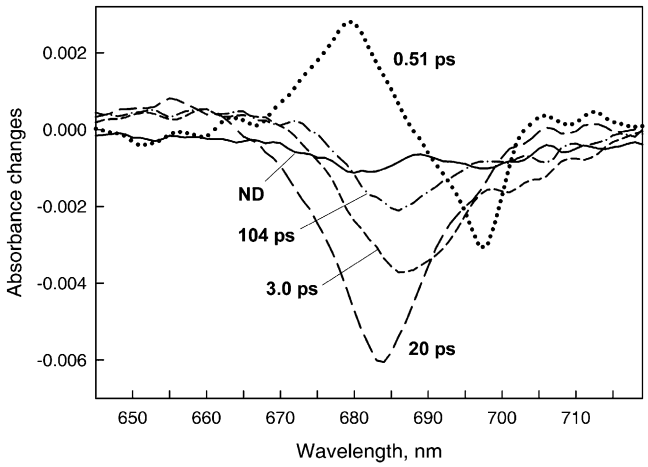

Figure 4. Decay associated spectra (DAS) obtained after global analysis of the transient kinetics detected in the PSI−LHCI supercomplex at room temperature and excitation at 700 nm. Kinetic processes are resolved on the 10 (A) and 210 ps time scales (B). See text for details.

Figure 4) has a conservative shape characteristic of an uphill energy transfer (see positive amplitudes at 680 nm) from Chls absorbing around 700 nm in the PSI−LHCI.

The spectral width of the 3.0 ps DAS indicates a complex nature of this kinetic phase. A nonconservative shape of the DAS suggests the predominance of the excitation decay processes over spectral shifts. We suggest that the shape of the spectrum could be explained by a combination of the excitation decay due to uphill energy transfer/excitation equilibrium and singlet−singlet annihilation, which is difficult to completely avoid for the PSI−LHCI supercomplex with large numbers of pigments. Transient absorption spectra in Figure 2 indicate that 1 out of every 50 pigments is excited by a laser pulse. As the total number of the pigments in the PSI−LHCI is 215 (95 Chl *a* in the PSI core + 40 Chl *b* + 80 Chl *a* in the LHCI as estimated in ref 12), this would account for 3.5 excitations created by a single laser flash. The Chl *b* molecules are not susceptible to excitation annihilation because they do not absorb in the 670−700 nm region. With the exclusion of 40 Chl *b* molecules, 95 Chl *a* of the PSI core and 80 Chl *a* of the LHCI are located in two different structural domains, which are energetically weakly coupled (see Discussion). This would result in a ~2-fold decrease in a probability of the annihilation (roughly less than two excitations per pulse). By modeling the shape of the 2−3 ps DAS observed in the study, we estimate that the annihilation could account for less than 50% of the observed spectrum.

The dominating kinetic phase in the PSI−LHCI supercomplex has the lifetime and the spectral shape that is experimentally well-established for the photochemical trapping in the PSI core antenna from *C. reinhardtii*.[13,18,41] The shape of this DAS is independent of the excitation wavelength and represents a fully equilibrated state of the PSI core. It should be noted that this equilibrated state does not involve any low-energy-absorbing forms around 700 nm, in contrast to the photochemical trapping DAS in cyanobacteria, where the clusters of the red pigments in the PSI core are involved in the excitation decay process.[3,4] A 104 ps DAS in Figure 4 is additional to the photochemical trapping in the PSI core (20 ps DAS) and indicates a decay of the photobleaching centered around 683 nm with a spectral shoulder extending to the red region.

The DAS of the long-lived kinetic components (nondecaying (ND) on the time scale of the study) represents the P700

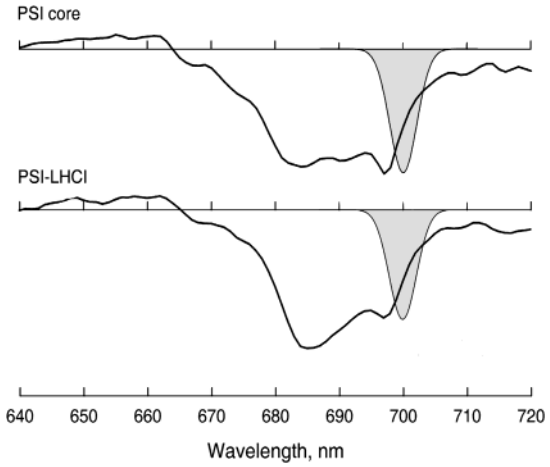

Figure 5. Comparison of the early time transient absorption difference spectra of the PSI core and the PSI−LHCI detected at 284 fs after the excitation at 700 nm. Also shown is the spectral profile of the excitation (fwhm = 5 nm).

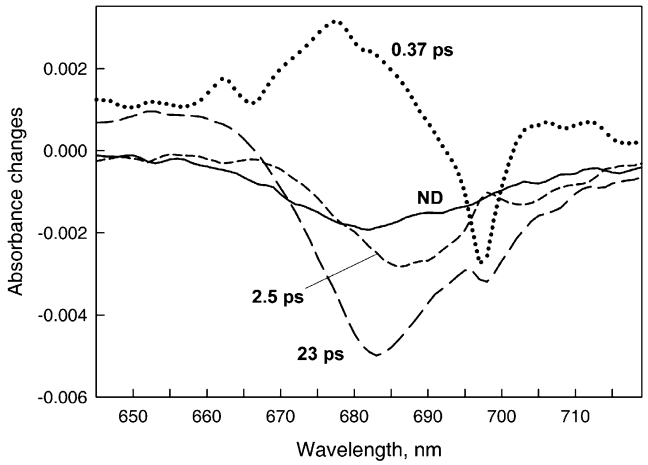

Figure 6. Decay associated spectra obtained after global analysis of the transient kinetics detected in the PSI core antenna on the 100 ps time scale at room temperature and excitation at 700 nm. The data are best fit with four exponential components with lifetimes of 0.37, 2.5, 23, and longer than 100 ps (nondecaying component). The latter component represents the sum of the long-lived P700 photooxidation and energetically uncoupled pigment−protein complexes. See text for details.

photooxidation overlapped with some processes of the slower excitation decay in the peripheral antenna (see ND spectra in Figure 4). A broad photobleaching band centered at 697 and at 680 nm as well as a trough in ΔA around 690 nm is characteristic of photooxidation of the primary donor in PSI from *C. reinhardtii*. We note that the maximum of ΔA of P700 in cyanobacterial PSI is located at 703 nm. The processes that are comparable with the lifetime of the $P700^+$ might include a long-lived excited antenna state around 680 nm and 700−710 nm (see ND spectrum in Figure 4). The lifetimes of these components are uncertain in the transient absorption study but can be resolved by picosecond fluorescence (see below).

Transient Absorption Changes of the PSI Core Particles. Similar transient absorption experiments were performed with the PSI core particles isolated from the PSI−LHCI supercomplexes by using mild detergent treatment (see Materials and Methods). We found that the transient absorption difference spectra of the PSI−LHCI (Figure 2) are largely similar to those in the PSI core detected under excitation at 700 nm (data not shown). This similarity is a consequence of the severe spectral overlap of the absorption spectra of Chl *a* in the PSI core and the LHCI. Comparison of the early transient absorption difference spectra of the PSI core and the PSI−LHCI supercomplex (Figure 5) confirms that the broad spectral features in both spectra originate from the excitonic interactions in the PSI core, while the decreased $\Delta A_{697}/\Delta A_{685}$ ratio in the 284 fs spectrum of the PSI−LHCI results from the overlap of the PSI core process with the uphill energy transfer to the bulk Chl *a* in LHCI.

Results of a four-component global fitting of the kinetic curves with free parameters are shown in Figure 6. DAS of the kinetic processes with lifetimes of 0.37, 2.5, and 23 ps largely exhibit the spectral features of the DAS detected for the PSI−LHCI (Figure 4). The differences include a well-defined shoulder at 700−710 nm in the 23 ps DAS (Figure 6), which is absent in the 20 ps DAS in Figure 4.

On the longer time scale, a nondecaying component represents an overlap of the P700 photooxidation and long-lived decay of energetically uncoupled pigments (around 680 nm). We would like to stress that depletion of the LHCI from the PSI−LHCI supercomplexes using mild detergent treatment probably results in some disturbance of the PSI core surface and accumulation of some energetically uncoupled pigments (see Discussion). The lifetime of these processes is uncertain in transient absorption experiments; however, it can be easily monitored by time-resolved fluorescence spectroscopy (see below).

Picosecond Fluorescence Spectroscopy of the PSI−LHCI and PSI Core at Room Temperature. To confirm the presence of an additional excitation trapping component in the PSI−LHCI supercomplex that originates from the structural coupling of the LHCI to the PSI core antenna, we analyzed the picosecond fluorescence decay in both PSI−LHCI and the PSI core particles at room temperature with nonselective excitation at 600 nm. The spectral profile of different phases of the fluorescence decay was obtained from the global analysis of the fluorescence kinetics detected on the time scale of 10 ns in the 640−780 nm spectral region with 5 or 10 nm steps. Experiments showed that the fluorescence decay of the PSI−LHCI supercomplex is characterized by a sum of the exponential components with lifetimes of 35 ± 5 ps, 107 ± 24 ps, 1.8 ± 0.1 ns, and 6.3 ± 1.1 ns. The exponential components of the fluorescence decay processes in the PSI core have lifetimes of 26 ± 3 ps, 204 ± 20 ps, 1.6 ± 0.5 ns, and 5.5 ± 0.9 ns. Figure 7 illustrates fluorescence decay associated spectra (FDAS) resulting from a four-component global fit of the emission kinetics of the PSI−LHCI supercomplex (A) and the PSI core (B). Parts A and B of Figure 7 show that dominating fluorescence phases in both samples have different shapes of the FDAS. A 35 ps FDAS in PSI−LHCI has a maximum at 685 nm and a relatively narrow width (fwhm = 30 nm). The latter is associated with increased F685/F720 ratio as compared to that in the 26 ps-FDAS in the PSI core (Figure 7B). These spectral changes correlate with increased antenna size in the PSI−LHCI and indicate an additional fluorescence decaying process, which is different from the photochemical trapping in the PSI core (see 26 ps DAS). This process as well as the phase of the fluorescence decay with a lifetime of 107 ps (Figure 7A), which appears in the fluorescence kinetics of the PSI−LHCI, is likely to originate in the LHCI peripheral antenna, which is energetically coupled to the PSI core. Similar results were obtained using transient absorption spectroscopy (see 104 ps DAS in Figure 4). The decreased F685/F720 ratio in the 107 ps FDAS indicates involvement of the low-energy fluorescence forms (690−720 nm), which is likely to appear as a result of the structural coupling of the LHCI to the PSI core. The 26 ps FDAS in the

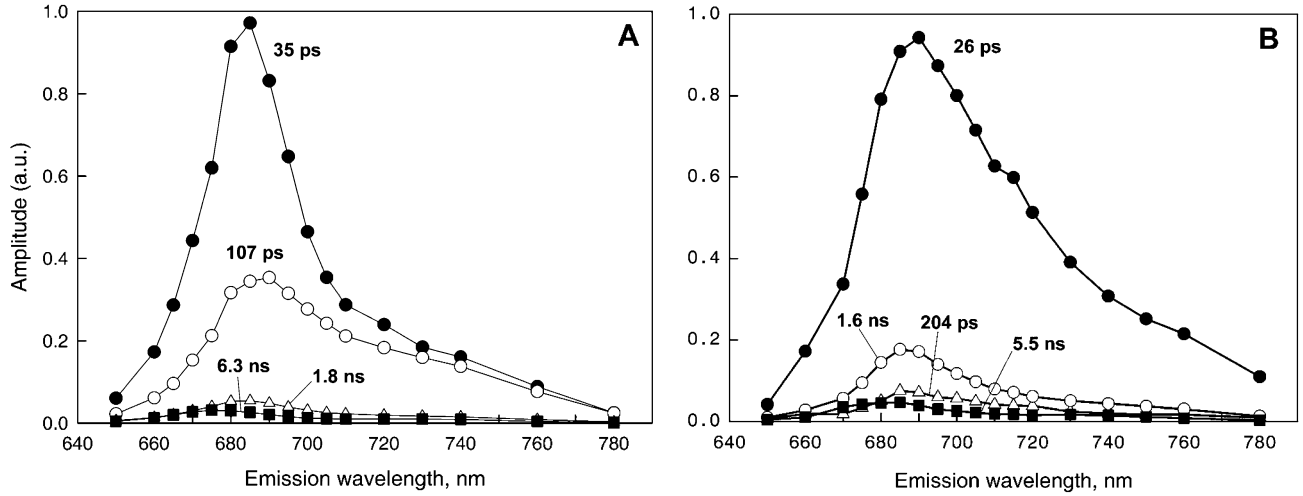

Figure 7. Fluorescence decay associated spectra (FDAS) obtained after global analysis of the fluorescence decay kinetics detected at room temperature under excitation at 600 nm in the PSI−LHCI (A) and the PSI core (B). Global χ^2 parameters are 1.048 and 1.012 for parts A and B, respectively.

PSI core reflects the overall excitation decay in the core antenna due to photochemical trapping. The spectrum indicates a major fluorescence band with maximum at 690 nm and a series of fluorescence spectral forms with substantial contribution around 720 nm that extends to the red spectral region. The red fluorescing species determine the width of the 26 ps-FDAS (fwhm = 60 nm).

Less than 7% of the fluorescence decay in the PSI−LHCI belongs to the processes with nanosecond lifetimes presented by 1.8 ns FDAS (uncoupled pigment−protein complexes) and 6.3 ns FDAS (free pigments) (see Figure 7A). In the PSI core fluorescence the processes with residual amplitudes have lifetimes of 204 ps and 5.5 ns. The 1.6 ns DAS observed in the fluorescence decay of the PSI core originates from energetically uncoupled pigments (see Discussion for analysis of the nature of this phase).

Discussion

Excitation Dynamics in the PSI Reaction Center. The absorption spectra in Figure 1 demonstrate that depletion of the PSI−LHCI supercomplex from the peripheral antenna results not only in a decrease of Chl *b* absorption at 650 nm but also in a 2 nm blue spectral shift, indicating a lack of specific Chl *a* spectral forms in the PSI core as compared to the PSI−LHCI. Apparently, these low-energy (red) spectral forms originate from absorption of Chl *a* molecules in the LHCI. Major Chl *a* absorption bands of the Lhca proteins in higher plants center at 676−680 nm with red pigments absorption extending to 710 nm, depending on the specific type of the Lhca.[27] These pigments significantly contribute to the red edge of the Q_y absorption band in higher plant PSI−LHCI,[32] in contrast to the absorption spectrum of the PSI−LHCI from *C. reinhardtii* used in our study (Figure 1, curve 1). Additionally, disruption of specific interactions of the PSI core and the LHCI might cause the observed changes in the red edge of the PSI core Q_y absorption band.

In the early transient ΔA spectra of both the PSI core and the PSI−LHCI (Figures 2A and 5), excitonic interactions among Chls of the PSI reaction center are manifested as the broad instantaneous photobleaching in the 670−700 nm region. Similar spectral features were reported earlier for the PSI core particles from *C. reinhardtii*.[34,41] Although the exciton coherence dominates the ΔA spectral changes at early times (within the duration of the laser pulse), excitation equilibration processes (uphill energy transfer) dominate the absorption changes at later times (as the exciton coherence should be lost after the excitation hopping takes place). The 0.37 ps DAS in the PSI core excitation dynamics (Figure 6) is characteristic of the uphill energy transfer processes in the core antenna. The broad shape of the rising part of the spectrum is due to overlapped equilibrated Chl *a* spectral forms of the heterogeneous Q_y absorption band of the PSI core antenna.[5]

The 2.5 ps DAS in the excitation dynamics of the PSI core characterizes the equilibration process that involves the long wavelength absorbing Chls along with the bulk antenna Chls. The absence of the rising part around 680 nm in the 2.5 ps DAS might be attributed to singlet−singlet annihilation, which constitutes at least 50% of the spectral changes (see Results). Excitation equilibration on the picosecond time scale was undoubtedly demonstrated for the cyanobacterial PSI core that possesses the red antenna pigments.[3,4] However, transient absorption spectroscopy studies of the PSI core from *C. reinhardtii*, reported on variation in the amount of the long-wavelength absorbing Chl *a* forms with the 2−4 ps antenna equilibration component being correlated with the presence of the red pigments.[13,18,34,41] Comparison of our data with the published reports allows us to suggest that the long wavelength absorbing Chls in the PSI core from *C. reinhardtii* are located on the periphery of the PSI core complex. These pigments are populated on the picosecond time scale and involved into the photochemical trapping as can be seen from the 23 ps DAS (Figure 6). Variation in the amount of the red Chl *a* species might result from accessibility of these pigments to different detergents, influence of isolation procedures as well as strain dependency.

The crystal structure of the PSI−LHCI from pea[2] revealed 93 Chls of the PSI core, 92 of which were in the same position as in the PSI core from cyanobacteria.[1] Significant positional modifications, however, were observed for the peripheral Chl B33 in the pea PSI. In the cyanobacterial PSI core, peripherally located Chls B33, B32, and B31 form a trimer assigned to the longest wavelength absorbing Chls.[1,5] Structural perturbations in the trimer in the eukaryotic PSI core might result in a less pronounced red spectral shift.

In contrast to the photochemical trapping in the PSI core (23 ps DAS in Figure 6), the trapping phase in the PSI−LHCI supercomplex (20 ps DAS in Figure 4) does not involve the red spectral forms. Such a discrepancy could be explained by

involvement of peripherally located red spectral forms of the core antenna into slower energy transfer processes resulted from structural association of the core antenna with the LHCI antenna. The spectral shape of the 104 ps DAS (Figure 4) observed in the excitation dynamics of the PSI−LHCI supercomplex supports this suggestion (see Discussion below).

We would like to stress that the biochemical purification of the PSI core particles from the PSI−LHCI in the strain of *C. reinhardtii* used in this study turns out to be a nontrivial task. Although the detailed structure of the PSI−LHCI from this green alga is unknown, the available structural model of the complex from pea[2] reveals extra ("gap") pigments on the interface of interacting LHCI and the PSI core, which might influence the excitation dynamics of the isolated PSI core particles. In particular, the shorter wavelength side of the long-lived decay components (ND spectrum in Figures 6 and 1.6 ns FDAS in Figure 7B) observed in the PSI core are likely to originate from energetically uncoupled pigments on the surface of the PSI core due to its possible disturbance upon depletion of the LHCI.

Excitation Energy Equilibration in the LHCI Antenna. Comparisons of the energy transfer components observed in the PSI−LHCI and the PSI core on the subpicosecond and picosecond time scales (Figures 4−6) reveal significant spectral overlap of the Chl *a* pools in the PSI core and the LHCI peripheral antenna. However, the early transient absorption spectra in the PSI−LHCI (Figure 5) demonstrate not only the instantaneous photobleaching due to excitonic interactions in the PSI core but also some additional ΔA changes that indicate the beginning of the process of excitation population of the Chl *a* species in the LHCI via uphill energy transfer. This process is described by the 0.51 ps DAS in Figure 4. In the isolated LHCI from higher plants Chl *a* spectral forms might be populated on the subpicosecond time scale via excitation of carotenoids,[30] Chl *b*, Chl *a*, and their broad vibronic bands.[39,42] Within picoseconds, the excitation redistributes among the major LHCI Chl *a* spectral forms with significant localization of the excitation on the red pigments in the 680−710 nm region.[3] Our recent time-resolved studies of the PSI−LHCI from *C. reinhardtii* with excitation of Chl *b* clearly identify this ultrafast excitation dynamics in the LHCI,[43] which is largely similar to the excitation dynamics induced by excitation of Chl *b* in isolated LHCI from higher plants.[3] The ultrafast energy transfer processes in the LHCI are governed by the Förster inductive-resonance mechanism, however, the excitation equilibration involves also the Chl *a* molecules, part of which are involved in pigment−pitment interactions (red pigments).[44] We note that excitonic interactions in the LHCI could contribute to the width of observed early transient spectra measured in PSI−LHCI (Figures 2A and 5). However, experimental reports on time-resolved spectroscopy of isolated LHCI from *Chlamydomonas* are unavailable.

A changed F680/F720 ratio in the 35 ps DAS detected in the PSI−LHCI (Figure 7A) most likely reflects combined photochemical trapping in the PSI core and the fluorescence decay in the LHCI peripheral antenna. Nonselective excitation at 600 nm used in picosecond fluorescence experiments (Figure 7) induces population of the major Chl *a* spectral forms in the PSI core and the LHCI via ultrafast relaxation (within 300 fs[42]) of broad vibronic bands of Chls (Figure 1). The decay of the excitation of the bulk Chl *a* in the LHCI dimers was shown to be biphasic and associated with energy equilibration within Chl *a* spectral forms on the picosecond time scale and the inter-subunit energy transfer with lifetimes in the range of 15−40 ps.[29,30]

Slow Excitation Decay in the PSI−LHCI Supercomplex. The data obtained by using transient absorption (Figures 4 and 6) and picosecond fluorescence spectroscopy (Figure 7) independently provide evidence for the additional excitation decay component in the PSI−LHCI with a lifetime of ∼100 ps. Comparison with the excitation dynamics in the PSI core clearly indicates that such a kinetic phase originates from the structural coupling of the LHCI peripheral antenna to the PSI core in the green alga *C. reinhardtii*. Similar kinetic phases have been observed by picosecond fluorescence spectroscopy in PSI-200 particles from *Arabidopsis thaliana*.[17] However, the shape of the 115−120 ps fluorescence DAS detected by Ihalainen and co-workers undoubtedly demonstrates involvement of significantly larger amounts of the red pigments in the process of the photochemical trapping in the PSI−LHCI from higher plants while the 104 ps DAS in Figure 4 and the 107 ps FDAS in Figure 7A have maxima at 680−690 nm. This difference might be caused by a changed composition of the LHCI peripheral antenna in *C. reinhardtii* (see below).

Recent biochemical and mutational studies of the LHCI from higher plants came to a conclusion that every type of the Lhca proteins in the peripheral antenna possesses the low-energy-absorbing Chls.[27,28,45] Pigment−pitment interactions of the Chls bound by the first and the second transmembrane helices in the LHCI are thought to be responsible for the red spectral shifts in absorption and the fluorescence.[27,44,45] Although LHCI in green algae seems to be similar to those isolated from higher plants, there are apparent but yet unstudied differences in molecular organization that causes these differences. Data of the present study suggest that the PSI−LHCI supercomplex from *C. reinhardtii* binds significantly fewer low-energy pigments than in higher plants.[27,32] Analysis of the time-resolved ΔA spectra infers that these pigments as well as the peripherally located red pigments in the PSI core absorb in the same spectral region (700−710 nm) and are involved in the slower energy transfer in the supercomplex.

The LHCI antenna in *C. reinhardtii* is diverse and contains seven to nine different Lhca proteins.[46−48] Proteomics studies suggests that the Lhca1 protein might be a dominant LHCI protein in the peripheral antenna of the PSI supercomplex in green algae.[46,47] In higher plants, Lhca1 proteins were suggested to bind red-shifted pigments, absorbing, however, in the 685−700 nm region in contrast to low-energy pigments in Lhca4 and Lhca3 absorbing further to the red.[27,45] If assume that the spectral properties of the Lhca1 in higher plants and green algae are similar, this could explain observation of the 715 nm peak of the 77 K fluorescence in the PSI−LHCI from *C. reinhardtii*[12] as compared to the maximum at 735 nm in the PSI−LHCI from higher plants.[32] Isolated LHCI polypeptides from *C. reinhardtii* were shown to contribute to 77 K fluorescence peak at 705 nm.[37] It was suggested[12,31] that the spectral properties of the peripheral antenna (particularly in *Chlamydomonas*) change upon association with the PSI core. In the PSI−LHCI supercomplex these changes are manifested as the red shift of the fluorescence from 705 nm (isolated LHCI) to 715 nm (PSI−LHCI supercomplex). Recent analysis of the excitation wavelength-dependent equilibration among the Chl *a* spectral forms in the PSI−LHCI at 77 K clearly identified a distinct ΔA band at 703 nm originating from the rise of photobleaching on the picosecond time scale (3−5 ps) in LHCI.[43]

At present a detailed structural model of the PSI−LHCI supercomplex from green algae is unavailable. We cannot rule out that the low-energy pigments in the PSI−LHCI from *C. reinhardtii* might be located between the layer of the LHCI and

PSI core surface as was suggested for the higher plant holocomplex crystal structure.[2] The spectral shape of the DAS with lifetime of 100−150 ps in the PSI−LHCI reveals some excitation wavelength dependence,[43] suggesting that the excited state in the supercomplex is not completely equilibrated on this time scale in agreement with the diffusion-limited model of the excitation dynamics. We note that this kinetic phase in the experiments with different excitation wavelengths displays heterogeneity, whose origin might be associated with the "gap" Chls found in the "cleft" between the LHCI belt and the PSI core.[2]

Peripheral LHCI Antenna Isoenergetic to the PSI Core in *C. reinhardtii*. The experimental data presented in this paper allow us to conclude that, in *Chlamydomonas*, the antennae of both the PSI core and the LHCI complex are isoenergetic, since the observed time-resolved absorption and fluorescence changes for both PSI core and the PSI−LHCI supercomplexes occur in the same spectral region (680−700 nm), which is determined by a severe spectral overlap of the Chl *a* spectral forms within the Q_y transition band (Figure 1). As recently reported,[12] the PSI−LHCI supercomplex from *C. reinhardtii* binds ∼40 Chl *b* and ∼175 Chl *a* molecules including ∼95 Chl *a* in the PSI core antenna and ∼80 Chl *a* in the LHCI.

For isoenergetic PSI core and LHCI with largely similar pools of Chl *a*, excitation of the PSI−LHCI supercomplex at 700 nm would result in a similar probability of excitation of either primary donor in the PSI core (absorbing at 697 nm) or low-energy Chls in the LHCI (red pigments) that presumably absorb in this spectral region. The excitation of the low-energy pigments populates the major spectral forms of Chl *a* in the LHCI via subpicosecond uphill energy transfer. This excitation equilibrates in the same spectral region as the excitation within the PSI reaction center. The observed ∼100 ps excitation decay phase in the PSI−LHCI supercomplex from green algae is in striking contrast to the energetically well coupled CP43′−PSI supercomplexes from iron−stress-induced cyanobacteria.[19] In the cyanobacterial supercomplex ∼290 Chl *a* molecules contribute to the absorption band at 673 nm while the pigments of the PSI reaction center including P700 absorb at 685−710 nm. Such a redistribution of the Chl *a* spectral forms amplified by an increase in light-harvesting capacity determines an efficient energy gradient from the peripheral antenna (CP43′) toward the PSI reaction center. Our data show that in the PSI−LHCI supercomplex ∼80 Chl *a* molecules in the peripheral antenna and ∼95 Chl *a* molecules of the PSI core have similar redistribution of the Chl *a* spectral forms; i.e., the LHCI antenna is isoenergetic to the PSI core.

In conclusion, on the basis of our experimental data and available structural models of the PSI−LHCI from higher plants[2] and green algae,[11,12] we suggest that the following factors could contribute to appearance of the slow 80−100 ps decay component in the excitation dynamics of the PSI−LHCI. Slow equilibration processes in the LHCI peripheral antenna such as intersubunit energy transfer[29,30] could significantly limit the overall decay of the excitation in the energetically coupled LHCI. The 4.4 Å resolution crystal structure of the PSI−LHCI from pea[2] identified asymmetry in the strength of the structural connections between the LHCI and the PSI core. A bottleneck step in the excitation equilibration within LHCI could induce a kinetic heterogeneity resulting from a fast (via "gap" pigments in the regions with tight contacts) and slow (via regions with weaker structural coupling). Since the core antenna and the peripheral antenna are isoenergetic, the observed slow equilibration time is determined by the ratio of the direct and back energy transfer in the slow pathway. The fast energy transfer processes from the peripheral antenna toward the PSI reaction center via tight structural connections are likely to be masked by the photochemical trapping phase in the PSI core (20−30 ps). Structure-based modeling will help to identify these specific pathways. Additional kinetic heterogeneity in the LHCI peripheral antenna from *C. reinhardtii* might originate from loosely bound LHCI polypeptides within the peripheral antenna. Low-resolution structural models suggest a larger size of the peripheral antenna in the LHCI−PSI supercomplex from *Chlamydomonas*[11,12] than in the higher plant PSI−LHCI.[2]

Acknowledgment. The authors would like to thank Jun Minagawa for donation of the His-tagged psbD mutant of *C. reinhardtii*. This work was supported by NRICGP/USDA Grant 2003-35318-13665 to A.N.M., NSF Grant MCB 0091250 to R.E.B., and a BBSRC grant to J.B. and J.K. This is publication no. 592 of the Center for the Study of Early Events in Photosynthesis at ASU.

References and Notes

(1) Jordan, P.; Fromme, P.; Witt, H. T.; Klukas, O.; Saenger, W.; Krauss, N. *Nature (London)* **2001**, *411*, 909.
(2) Ben-Shem, A.; Frolow, F.; Nelson, N. *Nature (London)* **2003**, *426*, 630.
(3) Melkozernov, A. N. *Photosynth. Res.* **2001**, *70*, 129.
(4) Gobets, B.; van Grondelle, R. *Biochim. Biophys. Acta* **2001**, *1507*, 80.
(5) Byrdin, M.; Jordan, P.; Krauss, N.; Fromme, P.; Stehlik, D.; Schlodder, E. *Biophys. J.* **2002**, *83*, 433.
(6) Sener, M. K.; Lu, D.; Ritz, T.; Park, S.; Fromme, P.; Schulten, K. *J. Phys. Chem. B* **2002**, *106*, 7948.
(7) Grossman, A. R.; Bhaya, D.; He, Q. *J. Biol. Chem.* **2001**, *276*, 11449.
(8) Gantt, E.; Grabowski, B.; Cunningham, F. X. Jr. *Light-harvesting antennas*; Green, B. R., Parson, W. W., Eds.; Kluwer Academic Publishers: Dordrecht, The Netherlands, 2003; pp 307−322.
(9) Bibby, T. S.; Nield, J.; Barber, J. *Nature (London)* **2001**, *412*, 743.
(10) Boekema, E. J.; Hifney, A.; Yakushevska, A. E.; Piotrowski, M.; Keegstra, W.; Berry, S.; Michel, K. P.; Pistorius, E. K.; Kruip, J. *Nature* **2001**, *412*, 745.
(11) Germano, M.; Yakushevska, A.; Keegstra, W.; van Gorkom, H. J.; Dekker: J. P.; Boekema, E. J. *FEBS Lett.* **2002**, *525*, 121.
(12) Kargul, J.; Nield, J.; Barber, J. *J. Biol. Chem.* **2003**, *278*: 16135.
(13) Hastings, G.; Hoshina, S.; Webber, A. N.; Blankenship, R. E. *Biochemistry* **1995**, *34*, 15512.
(14) White, N. T. H.; Beddard, G. S.; Thorne, J. R. G.; Feehan, T. M.; Keyes, T. E.; Heathcote, P. *J. Phys. Chem.* **1996**, *100*, 12086.
(15) Turconi, S.; Weber, N.; Schweitzer, G.; Strotmann, H.; Holzwarth, A. R. *Biochim. Biophys. Acta* **1994**, *1187*, 324.
(16) Croce, R.; Dorra, D.; Holzwarth, A. R.; Jennings, R. C. *Biochemistry* **2000**, *21*, 6341.
(17) Ihalainen, J. A.; Jensen, P. E.; Haldrup, A.; van Stokkum, I. H. M.; van Grondelle, R.; Scheller, H. V.; Dekker: J. *Biophys. J.* **2002**, *83*, 2190.
(18) Melkozernov, A. N.; Lin, S.; Su, H.; Bingham, S.; Webber, A. N.; Blankenship, R. E. *Biochemistry* **1997**, *36*, 2898.
(19) Melkozernov, A. N.; Bibby, T. S.; Lin, S.; Barber, J.; Blankenship, R. E. *Biochemistry* **2003**, *42*, 3893.
(20) Fromme, P.; Jordan, P.; Krauss, N. *Biochim. Biophys. Acta* **2001**, *1507*, 5.
(21) Scheller, H. V.; Jensen, P. E.; Haldrup, A.; Lunde, C.; Knoetzel, J. *Biochim. Biophys. Acta* **2001**, *1507*, 41.
(22) Jensen, P. E.; Haldrup, A.; Rosgaard, L.; Scheller, H. V. *Physiol. Plant.* **2003**, *119*, 313.
(23) Fromme, P.; Melkozernov, A. N.; Jordan, P.; Krauss, N. *FEBS Lett.* **2003**, *555*, 40.
(24) Boekema, E. J.; Jensen, P. E.; Schlodder, E.; van Breemen, J. F. L.; van Roon, H.; Scheller, H. V.; Dekker, J. P. *Biochemistry* **2001**, *40*, 1029.
(25) Tjus, S. E.; Roobol-Boza, M.; Pålsson, L.-O.; Andersson, B. *Photosynth. Res.* **1995**, *45*, 41.
(26) Schmid, V. H. R.; Cammarata, K. V.; Bruns, B. U.; Schmidt, G. W. *Proc. Natl. Acad. Sci U.S.A.* **1997**, *94*, 7667.

(27) Croce, R.; Morosinotto, T.; Castelletti, S.; Breton, J.; Bassi, R. *Biochim. Biophys. Acta* **2002**, *1556*, 29.
(28) Ganeteg, U.; Strand, A.; Gustafsson, P.; Jansson, S. *Plant Physiol.* **2001**, *127*, 150.
(29) Melkozernov, A. N.; Schmid, V.; Schmidt, G. W.; Blankenship, R. E. *J. Phys. Chem. B* **1998**, *104*, 8183.
(30) Gobets, B.; Kennis, J. T. M.; Ihalainen, J. A.; Brazzoli, M.; Croce, R.; van Stokkum, I. H. M.; Bassi, R.; Dekker, J.; van Amerongen, H.; Fleming, G. R.; van Grondelle, R. *J. Phys. Chem. B* **2000**, *105*, 10132.
(31) Knoetzel, J.; Bossmann, B.; Grimme, L. H. *FEBS Lett.* **1998**, *436*, 339.
(32) Jennings, R. C.; Zucchelli, G.; Croce, R.; Garlaschi, F. *Biochim. Biophys. Acta* **2003**, *1557*, 91.
(33) Rivadossi, A.; Zucchelli, G.; Garlaschi, F. M.; Jennings, R. C. *Photosynth. Res.* **1999**, *60*, 209.
(34) Müller, M. G.; Niklas, J.; Lubitz, W.; Holzwarth, A. R. *Biophys. J.* **2003**, *85*, 3899.
(35) Sugiura, M.; Inoue, Y.; Minagawa, J. *FEBS Lett.* **1998**, *426*, 140.
(36) Croce, R.; Zucchelli, G.; Garlaschi, F. M.; Jennings, R. C. *Biochemistry* **1998**, *37*, 17355.
(37) Bassi, R.; Soen, S. Y.; Frank, G.; Zuber, H.; Rochaix, J.-D. *J. Biol. Chem.* **1992**, *267*, 25714.
(38) Melkozernov, A. N.; Lin, S.; Blankenship, R. E. *Biochemistry* **2000**, *39*, 1489.
(39) Melkozernov, A. N.; Lin, S.; Schmid, V.; Paulsen, H.; Schmidt, G. W.; Blankenship, R. E. *FEBS Lett.* **2000**, *471*, 89.
(40) Gobets, B.; van Stokkum, I. H. M.; Rögner, M.; Kruip, J.; Schlodder, E.; Karapetyan, N. V.; Dekker: J. P.; van Grondelle, R. *Biophys. J.* **2001**, *81*, 407.
(41) Gibasiewicz, K.; Ramesh, V. M.; Melkozernov, A. N.; Lin, S.; Woodbury, N. W.; Blankenship, R. E.; Webber, A. N. *J. Phys. Chem. B* **2001**, *105*, 11498.
(42) Melkozernov, A. N.; Lin, S.; Schmid, V. H. R.; Lago-Places, E.; Paulsen, H.; Blankenship, R. E. In *PS 2001 Proceedings on the 12th International Congress on Photosynthesis*; Larkum, T., Osmond, B., Eds.; CSIRO Publishing: Brisbane, Australia; 2001; p S31−003.
(43) Melkozernov, A. N.; Kargul, J.; Lin, S.; Barber, J.; Blankenship, R. E. Manuscript in preparation.
(44) Melkozernov, A. N.; Blankenship, R. E. *J. Biol. Chem.* **2003**, *278*, 44542.
(45) Schmid, V. H. R.; Potthast, S.; Wiener, M.; Bergauer, V.; Paulsen, H.; Storf, S. *J. Biol. Chem.* **2002**, *277*, 37307.
(46) Hippler, M.; Klein, J.; Fink, A.; Allinger, T.; Hoerth, P. *Plant J.* **2001**, *28*, 595.
(47) Stauber, E. J.; Fink, A.; Markert, C.; Kruse, O.; Johanningmeier, U.; Hippler, M. *Eukaryot. Cell* **2003**, *2*, 978.
(48) Tokutsu, R.; Teramoto, H.; Takahashi, Y.; Ono, T.; Minagawa, J. *Plant Cell Physiol.* **2004**, *45*, 138.